JCTC Journal of Chemical Theory and Computation

Theoretical Investigations of the Nature of Interaction of ClF with HF, H_2O, and NH_3

Junyong Wu, Jingchang Zhang, Zhaoxu Wang, and Weiliang Cao*

Institute of Modern Catalysis, Beijing University of Chemical Technology, State Key Laboratory of Chemical Resource Engineering, Beijing 100029, China

Received July 8, 2006

Abstract: The interactions of the first-row hydrides (HF, H_2O, and NH_3) with ClF have been investigated by performing calculations at the second-order perturbation theory based on the Møller−Plesset partition of the Hamiltonian with the aug-cc-pVTZ basis set. The geometries and vibrational frequencies in the present study were obtained by carrying out explicit counterpoise-corrected optimization. In order to understand that the Cl−X-type (X = F, O, and N) structure is more stable than the corresponding hydrogen-bonded structure in these complexes, the electronic properties were also investigated. Furthermore, the symmetry-adapted perturbation theory calculations were performed to gain more insight into the nature of the hydrogen-bond and Cl−X-type interactions. The analysis of the interaction energy components indicates that, in contrast to the hydrogen-bonded complexes, the inductive and dispersive interaction is the most important term in the Cl−X-type complexes, as we progress from HF to NH_3.

1. Introduction

The number of individual crystal structures, in which weak interactions have been reported to be important, has grown rapidly in recent years.[1−3] Therefore, understanding the nature of these intermolecular interactions is a necessary step toward a full rationalization of the packing and also a key preliminary step to design new crystals. By consideration that crystal packing results from the sum of many different contributions of directional and nondirectional intermolecular interactions, it is important that different types of interactions should be considered jointly in structure analysis. Recently, although research has traditionally focused on the more well-known hydrogen-bonded interactions,[3−6] a growing system of experimental and theoretical evidence confirms that interactions such as −X−Y− (X = F, Cl, Br, or I; Y = N, O, S or π) similarly play important roles in crystal engineering.[7−32]

Although the natures of hydrogen bonds and interactions of the −X−Y− type are different, it is still significant to compare the hydrogen bond with the interactions of the −X−Y− type. So in this paper, we investigated the nature of hydrogen bond and −X−Cl− type interactions of ClF with the first hydrides (HF, H_2O, and NH_3). We focused on the lowest interaction potential complexes of the investigated hydrogen-bonded and −X−Cl− type complexes. To further investigate the relative importance of electrostatic, dispersion, induction, and exchange-repulsion energies of these hydrogen-bonded and −X−Cl− type (also referred to in this paper as X−Cl-type) complexes, we have decomposed the interaction energies into these components using symmetry-adapted perturbation theory (SAPT).[33,34]

2. Theoretical Methods

All the results presented in this work were produced by employing either conventional supermolecular (SM) variational or SAPT methods.[33,34] Though the SM method is conceptually and computationally simple, it does not provide a clear picture of the interaction forces which are responsible for the interaction. On the other hand, the SAPT method computes the interaction energy directly as a sum of electrostatic, exchange-repulsion, induction, and dispersion contributions so that a physical interpretation of the interactions between the complex monomers can be evinced. The

* Corresponding author phone: +86 10 64444919; fax: +86 10 64434898; e-mail: caowl@mail.buct.edu.cn.

10.1021/ct600229n CCC: $37.00
Published on Web 12/10/2006

details of the calculations are briefly elaborated to aid in the discussion of the results.

2.1. Supermolecular Calculations. The second-order Møller-Plesset theory (MP2)[35] has been shown to be effective and accurate in determining the equilibrium structure and binding energy for many hydrogen-bonded and other weakly bonded complexes.[36] The basis set applied here is Dunning's correlation consisted basis set aug-cc-pVTZ.[37] The basis-set superposition error (BSSE) was eliminated by the standard counterpoise (CP) correction method of Boys and Bernardi.[38] Again, some authors claimed that the normal recipe of counterpoise correction of carrying out a single-point correction without further optimization could not find the correctly optimized structures and frequencies. They advocated that geometrical parameters, vibrational frequencies, and energies should be determined using explicit BSSE corrections.[39−42] So in the present study, ab initio structures of complexes were determined using counterpoise-corrected gradient optimization at the MP2(full)/aug-cc-pVTZ level. No symmetries were constrained in the optimization. Frequency calculations were performed to verify that the structures were minima on the potential energy surface. The BSSE-corrected vibrational frequencies and hence the zero-point vibrational energy (ZPVE) corrections were also evaluated for all complexes at the same theory level. The analysis went further with those obtained by means of the natural bond orbital (NBO) theory of Weinhold and co-workers.[43] The NBO analysis will allow us to quantitatively evaluate the charge transfer (CT) involving the formation of a hydrogen bond or halogen bond. All ab initio calculations were carried out with the Gaussian 03 suite of programs.[44] NBO analysis was conducted on the MP2-optimized structures, the Hartree−Fock (HF) densities, and the built-in subroutines of the Gaussian 03 program.

The performance of the all-electron MP2 method with the aug-cc-pVTZ basis set is examined by studying four small monomer molecules. The optimal bond lengths of HF and ClF calculated at the MP2(full)/aug-cc-pVTZ level are 0.9202 and 1.6346 Å, respectively, which is in very good agreement with the experimental values of 0.9170 and 1.6281 Å.[45] For water, the MP2(full)/aug-cc-pVTZ bond length of 0.9590 Å and bond angle of 104.2° compare well with the experimental bond length of 0.9555 Å and bond angle of 104.5°.[45] For ammonia, the MP2(full)/aug-cc-pVTZ bond length of 1.0098 Å and bond angle of 106.8° also compare well with the experimental bond length of 1.0120 Å and bond angle of 106.7°.[45]

2.2. SAPT Calculations. In this study, the SAPT calculations reported here used the correlation level technically designated as SAPT2, and they were carried out using the aug-cc-pVTZ basis set at the MP2(full)/aug-cc-pVTZ geometry. The SAPT interaction energy can be represented as $E_{int} = E_{int}^{HF} + E_{int}^{CORR}$, where E_{int}^{HF} is the sum of all of the energy components evaluated at the Hartee−Fock level and E_{int}^{CORR} is the sum of all of the energy components evaluated at the corrected level. E_{int}^{HF} can be represented as

$$E_{int}^{HF} = E_{elst}^{(10)} + E_{exch}^{(10)} + E_{ind,resp}^{(20)} + E_{exch-ind,resp}^{(20)} + \delta E_{int,resp}^{HF}$$

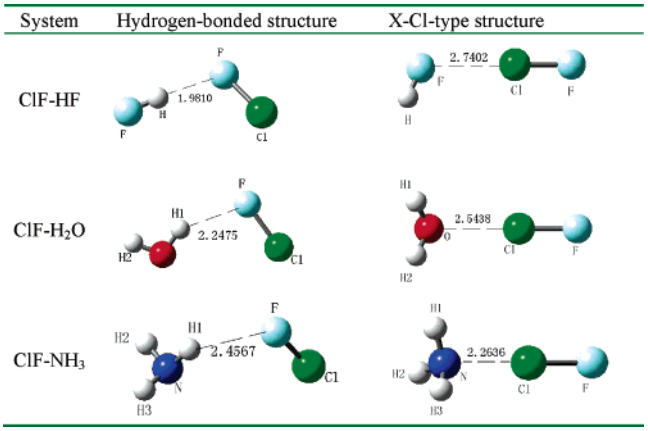

Figure 1. MP2(full)/aug-cc-pVTZ optimized low-energy structures (distances in Å). The dashed lines indicate noncovalent bond.

The superscript (*ab*) denotes orders in perturbation theory with respect to the intermolecular interaction operator and the intramolecular correlation operator, respectively. It can be seen from the above equation that the HF interaction energy includes first-order polarization and exchange and second-order induction and exchange-induction contributions. The subscript "resp" indicates that the induction and exchange-induction contributions include the coupled-perturbed HF response.[46] δE_{int}^{HF} contains the third- and higher-order HF induction and exchange induction contributions.

We have employed the SAPT2 approach, in which the correlative portion of the interaction energy E_{int}^{CORR} is nearly equivalent to the supermolecular MP2 correlation energy and can be represented as

$$E_{int}^{CORR} = E_{elst,resp}^{(12)} + E_{exch}^{(11)} + E_{exch}^{(12)} + {}^{t}E_{ind}^{(22)} + {}^{t}E_{exch-ind}^{(22)} + E_{disp}^{(20)} + E_{exch-disp}^{(20)}$$

Where ${}^{t}E_{ind}^{(22)}$ represents the part of $E_{ind}^{(22)}$ that is not included in $E_{ind,resp}^{(20)}$. A more detailed description of SAPT and some of its applications can be found in some recent references.[33,34,47−52] SAPT calculations were performed using the SAPT2002 program.[53]

3. Results and Discussion

3.1. Geometrical Parameters, Interaction Energies, and Vibrational Frequencies. The equilibrium geometries for the minimum energy hydrogen-bonded and X−Cl-type structures of ClF with the first hydrides (HF, H_2O, and NH_3) are displayed in Figure 1. Theoretical results for the interaction energies of these complexes are summarized in Table 1. Some selected geometrical parameters and vibrational frequencies are given in Tables 2 and 3.

Table 1 lists the interaction energies (ΔE), BSSE, interaction energies corrected for BSSE (ΔE^{CP}), ZPVE, interaction energies corrected for both BSSE and ZPVE ($\Delta E^{CP+ZPVE}$), and intermolecular distances (R_{int}) obtained at the MP2(full)/aug-cc-pVTZ level. The importance of the inclusion of electron correlation in the description of these complexes can be seen from the values of ΔE_{corr}. It is clear from Table

Table 1. Interaction Energies without (ΔE) and with (ΔE^{CP}) BSSE Correction and BSSE, ZPVE, and Interaction Energies for Both BSSE and ZPVE ($\Delta E^{CP+ZPVE}$)[a,b]

	ClF···HF	ClF···H_2O	ClF···H_3N	HF···ClF	H_2O···ClF	H_3N···ClF
ΔE	−3.066	−2.088	−1.627	**−2.844**	**−5.954**	**−12.623**
ΔE_{corr}	−1.733	−1.653	−1.471	**−1.537**	**−3.745**	**−11.184**
BSSE	1.055	0.792	0.689	**0.472**	**0.838**	**1.719**
ΔE^{CP}	−2.011	−1.296	−0.938	**−2.372**	**−5.116**	**−10.903**
ZPVE	1.077	0.763	0.493	**0.639**	**1.348**	**2.133**
$\Delta E^{CP+ZPVE}$	−0.934	−0.533	−0.445	**−1.733**	**−3.768**	**−8.770**
R_{int}	1.9810	2.2475	2.4567	**2.7402**	**2.5438**	**2.2636**

[a] All energies are in kcal/mol; ΔE_{corr} is determined from the difference between MP2 and HF binding energies (not corrected); R_{int} is the intermolecular distance. [b] Numbers in bold are values of the corresponding X−Cl-type complexes.

Table 2. Selected Geometrical Parameters (Å and deg), Frequencies (cm^{-1}), and IR Intensities (km/mol) of Hydrogen-Bonded Complexes Calculated at the MP2(full)/aug-cc-pVTZ Level[a]

			hydrogen-bonded complexes		
parameters	hydrogen-donor monomer	hydrogen-acceptor monomer	F−H···F−Cl	HO−H···F−Cl	H_2N−H···F−Cl
∠X−H···F			173.9	146.0	143.8
R(H···F)			1.9810	2.2475	2.4567
R(X−H)	0.9202 0.9590 1.0098		0.9229	0.9597	1.0099
ΔR(X−H)			0.0027	0.0007	0.0001
freq (X−H)	4135.3 (121.2) 845.7 (5.8) 532.9 (3.1)		4075.0 (349.6)	3841.6 (12.9)	3532.5 (5.9)
Δfreq (X−H)			60.3	4.10	0.40
R(Cl−F)		1.6346	1.6421	1.6392	1.6375
freq (Cl−F)		806.5 (27.8)	797.2 (33.8)	800.7 (31.0)	802.8 (30.6)

[a] X represents the F atom of HF, the O atom of H_2O, and the N atom of NH_3; values in parentheses are IR intensities.

Table 3. Selected Geometrical Parameters (Å and deg), Frequencies (cm^{-1}), and IR Intensities (in km/mol) of X−Cl-type Complexes Calculated at the MP2(full)/aug-cc-pVTZ Level[a]

		complexes with halogen acceptor		
parameters	halogen-donor monomer	FH	OH_2	NH_3
		FCl···XH_n		
∠F−Cl···X		178.1	179.8	180.0
R(Cl···X)		2.7402	2.5438	2.2636
R(Cl−F)	1.6346	1.6396	1.6507	1.7046
freq (Cl−F)	806.5 (27.8)	796.8 (42.3)	768.5 (84.2)	641.8 (227.5)
Δfreq (Cl−F)		9.7	38	164.7

[a] X represents the F atom of HF, the O atom of H_2O, and the N atom of NH_3; values in parentheses are IR intensities.

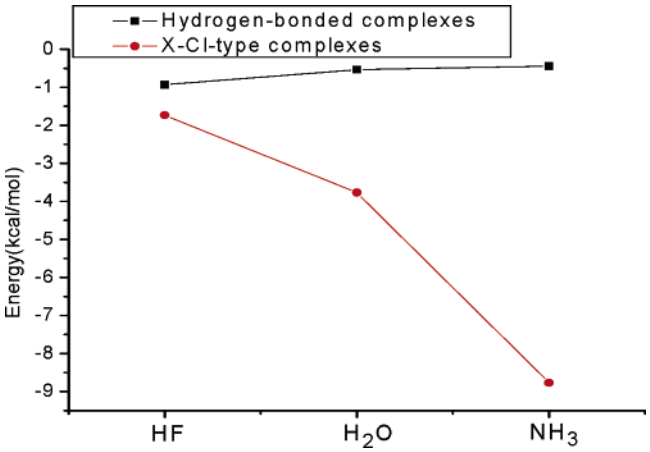

Figure 2. Comparison of the BSSE- and ZPVE-corrected interaction energies [MP2(full)/aug-cc-pVTZ] of all the hydrogen-bonded and X−Cl-type complexes.

1 that the interaction energies of these hydrogen-bonded minimum structures decrease in the order HF > H_2O > NH_3. This order is correlated to the electronegativity of the X atom of the hydride. On the contrary, the interaction energies of these corresponding X−Cl-type minimum structures increase in the order HF < H_2O < NH_3. This order is reasonable because the gas-phase basicity of the halogen atom acceptors is in the same order.

It is interesting to compare the hydrogen-bonded minimum structures (ClF−H_nX) with the corresponding X−Cl-type minimum structures (H_nX−ClF). The BSSE-uncorrected interaction energies (ΔE) of the hydrogen-bonded complex ClF−HF is larger than those for the corresponding X−Cl-type complex HF−ClF. However, the BSSE-corrected interaction energies (ΔE^{CP}) of the X−Cl-type structure HF−ClF are larger than those for the hydrogen-bonded structure ClF−HF by 0.361 kcal/mol. A plot of the ZPVE-corrected interaction energies of these complexes (Figure 2) evaluated at the MP2/(full)/aug-cc-pVTZ level reveals that all of the X−Cl-type complexes are more stable than the corresponding hydrogen-bonded complexes. The calculated interaction

Table 4. Natural Bond Orbital Analysis at the HF/aug-cc-pVTZ//MP2(full)/aug-cc-pVTZ Level (ΔE^2 in kcal/mol, $\Delta\epsilon$ in Hartree, Δq in Au)[a,b]

complexes	donor NBOs	δ	acceptor NBOs	δ	ΔE^2	$\Delta\epsilon$	Δq
ClF−H−F	F lone pair	1.992 (1.996)	H−F o˙ antibond	0.004 (0.000)	3.00	1.50	0.007
ClF−H−OH	F lone pair	1.994 (1.996)	H−O o˙ antibond	0.001 (0.000)	0.88	1.45	0.004
ClF−H−NH_2	F lone pair	1.995 (1.996)	H−N o˙ antibond	0.001 (0.000)	0.42	1.41	0.003
HF−Cl−F	F lone pair	1.993 (1.998)	Cl−F o˙ antibond	**0.005 (0.000)**	**2.57**	**1.07**	**0.004**
H_2O−Cl−F	O lone pair	1.973 (1.996)	Cl−F o˙ antibond	**0.022 (0.000)**	**9.17**	**0.94**	**0.020**
H_3N−Cl−F	N lone pair	1.857 (1.997)	Cl−F o˙ antibond	**0.119 (0.000)**	**48.32**	**0.75**	**0.130**

[a] Numbers in bold are values of the corresponding X−Cl-type complexes. [b] Data in the parentheses are the occupancies of the corresponding NBOs of the isolated molecules. Δq is the amount of charge transfer obtained by the natural population analysis (NPA).

energies of hydrogen-bonded complexes at the BSSE- and ZPVE-corrected levels lie in the −0.445 to −0.934 kcal/mol range, indicating a relatively weak hydrogen bond. In the case of X−Cl-type complexes, the interaction energies lie in the −1.733 to −8.770 kcal/mol range, indicating that the interactions are stronger. The greatest corrected intermolecular interaction in the dimers is −8.770 kcal/mol, belonging to the X−Cl-type complex, H_3N−ClF.

Table 2 shows that there is an elongation of the X−H and the Cl−F bonds upon hydrogen-bonded complex formation. The corresponding harmonic vibrational frequencies are also shown in Table 2. The frequency analysis shows the red-shifting character of the X−H−F interaction. In agreement with the computed X−H bond elongation, the X−H stretching frequencies are lower by 60.3−0.4 cm^{-1} in the complexes than the corresponding frequencies in the monomers. The individual red shift can be correlated directly to the magnitude of X−H bond elongations. In accordance with the interaction energies, the extent of the red shifts is shown to decrease in sequence from HF to NH_3.

Similarly, in the case of X−Cl-type complexes (FCl−XH_n), Table 3 shows that there is an elongation of the Cl−F bond upon complex formation. The corresponding harmonic vibrational frequencies and IR intensities are also shown in Table 3. The frequency analysis reveals the red-shifting character of the FCl−X interactions in the dimers. In agreement with the computed Cl−F bond elongation, the Cl−F stretching frequencies are lowered by 9.7−164.7 cm^{-1} in the complexes than the corresponding frequencies in the monomers. The individual red shift can be correlated directly to the magnitude of Cl−F bond elongations. In accordance with the interaction energies, the extent of the red shifts is shown to increase in sequence from HF to NH_3. As expected, the IR intensities behave in the same way.

3.2. NBO Analysis. For a better understanding of the interaction, a NBO analysis has been carried out at the HF/aug-cc-pVTZ level of theory using MP2(full)/aug-cc-pVTZ geometry. The occupancy (δ) of frontier molecular orbitals involving the CT between subsystems, the second-order perturbation energy lowering (ΔE^2) due to the interaction of donor and acceptor orbitals, and the difference ($\Delta\epsilon$) of energies between acceptor and donor NBOs, provided by NBO analysis, are collected in Table 4.

Table 5. Mulliken Charge Transfer from H_nX to ClF at the MP2/aug-cc-pVTZ and HF/aug-cc-pVTZ Level

complexes	Q_{CT} (au) MP2/aug-cc-PVTZ	Q_{CT} (au) HF/aug-cc-pVTZ
ClF···H−F	0.021	0.021
ClF···H−OH	0.014	0.014
ClF···H−NH_2	0.004	0.004
HF···Cl−F	0.009	0.009
H_2O···Cl−F	0.010	0.011
H_3N···Cl−F	0.112	0.115

Let us first repeat that the formation of a hydrogen-bonded complex involves CT from the proton acceptor to the proton donor. This results in the increase of electron density in the H−X antibonding orbitals of the proton donor. For the X−Cl-type, the case is a little similar.[42] The CT from the lone pairs of the electron donor in the halogen atom acceptor is mainly directed to the Cl−F antibonding orbitals of the halogen atom donor too. Because the CT accompanies the formation of hydrogen bonds or X−Cl bonds and plays a major role in it, ΔE^2 can be taken as an index to judge the strength of hydrogen bonds or X−Cl bonds. As can been see from Table 4, in the case of hydrogen-bonded complexes, the CT stabilization energies are computed to be 3.00, 0.88, and 0.42 kcal/mol for n(F)−o˙*(H−F), n(F)−o˙*(H−O), and n(F)−o˙*(H−N) interactions, respectively, which are comparable in magnitude to their interaction energies. For the X−Cl-type complexes, the charge-transfer stabilization energies are computed to be 2.57, 9.17, and 48.32 kcal/mol for n(F)−o˙*(Cl−F), n(O)−o˙*(Cl−F), and n(N)−o˙*(Cl−F) interactions, respectively, which are also comparable in magnitude to their interaction energies. The larger CT stabilization energies for the N−Cl-type complex H_3N−ClF confirm that it is a strong and partly covalent complex.

The result of the Mulliken charge transfer (Q_{CT}) is presented in Table 5. It is worth mentioning that the Mulliken charge transfer from H_nX to ClF takes place for all of the complexes. The amount of the Mulliken transferred charge is approximately equal at the MP2/aug-cc-pvTZ and HF/aug-cc-pVTZ levels.

3.3. SAPT Studies. To gain more insight the nature of the interaction, we further performed SAPT to analyze the interaction energy in terms of physically meaningful com-

Table 6. Partition of the Energies (kcal/mol) Derived from SAPT Calculations in Electrostatic (E_{elst}), Exchange (E_{exch}), Inductive (E_{ind}), and Dispersive (E_{disp}) Energies, as Defined by eqs 2−5[a,b]

	hydrogen-bond complexes			X−Cl-type complexes		
	ClF···HF	ClF···H_2O	ClF···H_3N	FCl···FH	FCl···OH_2	FCl···NH_3
E_{elst}	−2.456	−0.903	−0.926	**−3.404**	**−10.371**	**−36.666**
E_{exch}	2.539	0.963	1.257	**3.245**	**11.104**	**45.387**
E_{ind}	−1.072	−0.211	−0.169	**−0.602**	**−2.142**	**−12.199**
E_{disp}	−1.058	−1.120	−1.136	**−1.644**	**−3.740**	**−9.393**
E_{int}^{SAPT2}	−2.051	−1.271	−0.971	**−2.406**	**−5.148**	**−12.870**
$E_{int}^{(MP2)a}$	−2.011	−1.296	−0.938	**−2.372**	**−5.116**	**−10.903**

[a] MP2(full)/aug-cc-pVTZ counterpoise-corrected interaction energies. [b] Numbers in bold are values of the corresponding X−Cl-type complexes. All energies are in kcal/mol.

ponents such as electrostatic, induction, dispersion, and exchange energies.

The electrostatic component of the interaction energy is represented here by the sum of $E_{elst}^{(10)}$ and $E_{elst,resp}^{(12)}$. The induction contribution to the interaction energy is mainly contained in $E_{ind,resp}^{(20)}$. This is a second-order energy correction that results from the distortion of the charge distribution of one monomer by the electrostatic charge distribution of another monomer, and vice versa. This mutual polarization of the monomer by the static electric field of the other is the polarizabilities of the monomers. The leading intramonomer correlation contribution is concluded in ${}^tE_{ind}^{(22)}$ and accounts for only 2% of the induction energy. The attractive part of the induction energy is substantially quenched by the repulsive exchange-induction energy (represented by $E_{exch-ind,resp}^{(20)}$ and ${}^tE_{exch-ind}^{(22)}$). As noted by Jeziorski and co-workers,[33] any quantitatively accurate calculation of the induction energy cannot neglect the exchange-induction contribution. To simplify the analysis, for the present purposes, we have designated the exchange-dispersion and exchange-induction terms as dispersion and induction, respectively. So, the induction energy terms calculated here are $E_{ind,resp}^{(20)}$, ${}^tE_{ind}^{(22)}$, $E_{exch-ind,resp}^{(20)}$, and ${}^tE_{exch-ind}^{(22)}$. The dispersion energy is represented here by the sum of $E_{disp}^{(20)}$ and $E_{exch-disp}^{(20)}$, where $E_{disp}^{(20)}$ is the second-order dispersion energy, $E_{exch-disp}^{(20)}$ standing for the second-order correction for a coupling between the exchange repulsion and the dispersion energy. The exchange energy terms calculated here are $E_{exch}^{(10)}$, $E_{exch}^{(11)}$, $E_{exch}^{(12)}$, and $\delta E_{int,resp}^{HF}$. $E_{exch}^{(10)}$ accounts for the repulsion due to the Pauli exclusion principle and arises from the antisymmetry requirement of the wave function; $E_{exch}^{(11)}$ and $E_{exch}^{(12)}$ account for the effects of intramonomer correlation on the exchange repulsion. Therefore, The SAPT interaction energy, E_{int}, is given by

$$E_{int} = E_{elst} + E_{ind} + E_{disp} + E_{exch} \quad (1)$$

where

$$E_{elst} = E_{elst}^{(10)} + E_{elst,resp}^{(12)} \quad (2)$$

The SAPT-derived components of the interaction energy

$$E_{exch} = E_{exch}^{(10)} + E_{exch}^{(11)} + E_{exch}^{(12)} + \delta E_{int,resp}^{HF} \quad (3)$$

$$E_{ind} = E_{ind,resp}^{(20)} + {}^tE_{ind}^{(22)} + E_{exch-ind,resp}^{(20)} + {}^tE_{exch-ind}^{(22)} \quad (4)$$

$$E_{disp} = E_{exch-disp}^{(20)} + E_{disp}^{(20)} \quad (5)$$

are summarized in Table 6. It can be seen that the results of SAPT2 (E_{int}^{SAPT2}) are in good agreement with the results obtained at the MP2(full)/aug-cc-PVTZ level, suggesting that SAPT2/aug-cc-PVTZ is a proper method to study the intermolecular interactions in these studied complexes.

To elucidate the role of each term in the total interaction energy, we have plotted the magnitude of the individual interaction energy component (see Figure 3). Table 6 and Figure 3 show that the exchange energy is larger than the absolute value of the electrostatic energy for the three weak hydrogen-bonded complexes. The induction energy term and the dispersion energy term are nearly equal for the complex ClF−HF. For the ClF−H_2O and ClF−H_3N complexes, the induction energy is rather small, and the dispersion energy dominates. All of this is opposite of the decomposition for normal hydrogen bonds, which are known to be electrostatic in nature. Therefore, this type of interaction cannot be called conventional hydrogen bonding. The interaction may be considered as unconventional hydrogen bonding.

On the other hand, in the case of the X−Cl-type complexes, we find the electrostatic energies dramatically increase as we progress from HF to NH_3. The electrostatic interaction pulls the two monomers close to each other, which results in large values of all other energy components. For H_2O−ClF and H_3N−ClF, the exchange energy becomes even larger than the absolute value of the electrostatic energy, but the large attractive induction and dispersion energies lead to a very strong interaction. In the strongest X−Cl-type complex, H_3N−ClF, the induction energy is the most important attractive term, followed by the exchange and electrostatic energy, and is responsible for stabilizing the complex. This domination of the induction and exchange terms is the main feature of the strong and partly covalent bonds.

Additionally, the induction energy can be described to result from the interaction between the highest occupied molecular orbital and the lowest unoccupied molecular orbital. The inductive type of molecular orbital interaction can also be correlated to the extent of CT. It would be interesting to examine if the extent of charge transfer can be correlated to the total induction energy. We have carried out an analysis, using the charge transfer obtained by the natural population analysis (NPA) (Δq; Table 4). It can be seen from Figures 4 and 5 that, in the weak hydrogen-bonded

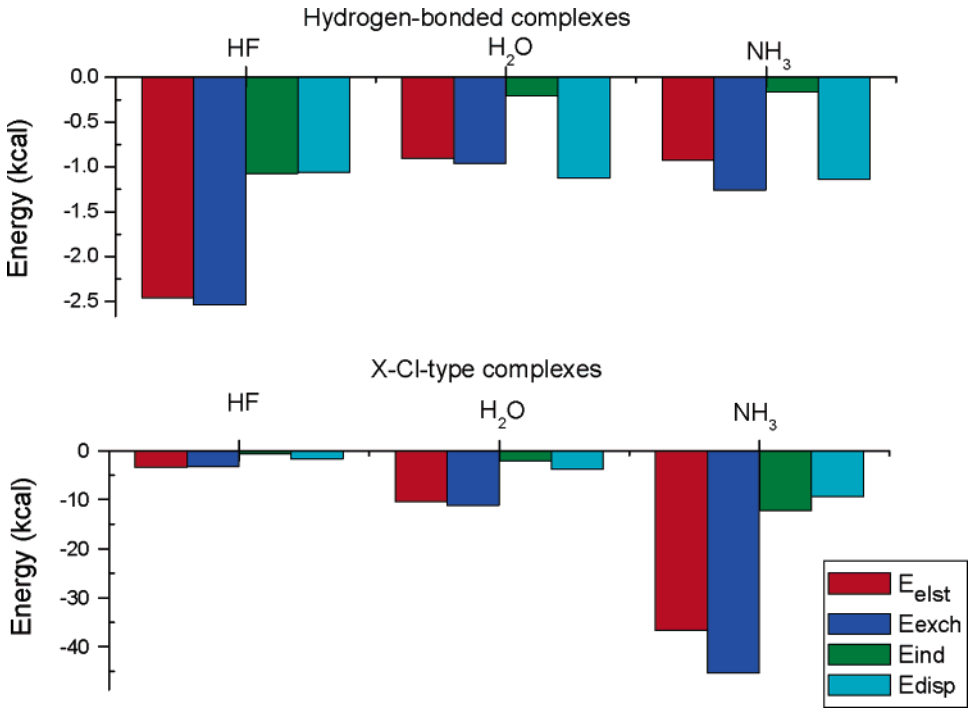

Figure 3. Bar plots of SAPT interaction energy components (E_{elst}, E_{ind}, E_{disp}, and E_{exch}) for the hydrogen-bonded complexes and X−Cl-type complexes according to eqs 1−5.

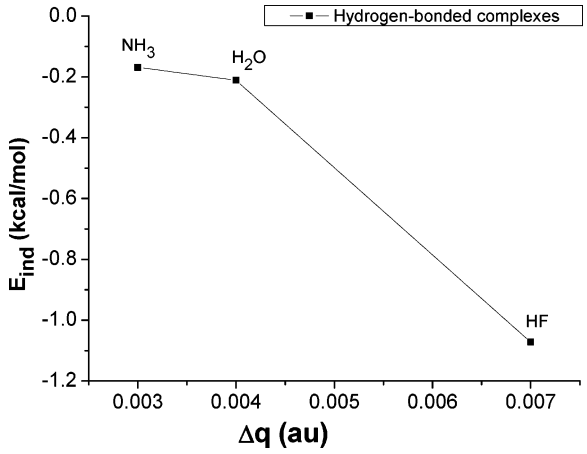

Figure 4. Correlation of the electronic charge transferred from ClF to the hydride with the total induction energy in the hydrogen-bonded complexes.

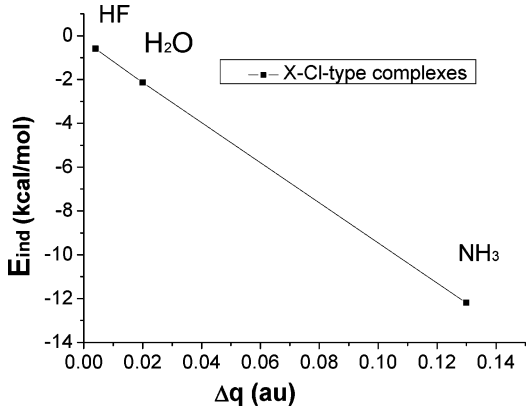

Figure 5. Correlation of the electronic charge transferred from the hydride to the ClF with the total induction energy in the X−Cl-type complexes.

complexes, a decrease in the magnitude of the charge transfer (Δq) from HF to NH_3 leads to a less induction energies. In the case of the X−Cl-type complexes, the charge-transfer correlates well with the total induction energies.

4. Conclusions

In summary, we have systematically investigated the interaction of the first-row hydrides with ClF. We also focused on the decomposition of the interaction energy into physically meaningful terms and on the basis of the parameters of molecular properties characterized and described the intermolecular interaction. Our results can be summarized as follows:

1. The total interaction energies of the X−Cl-type complexes are more stable than the corresponding weak hydrogen-bonded complexes. The charge-transfer analysis discloses the different physical properties of the weak hydrogen bond and X−Cl bond.

2. For all the investigated weak hydrogen-bonded complexes, the exchange energy outweighs the electrostatic energy, which is opposite of the decomposition for normal hydrogen bonds. This type of interaction may be considered as unconventional hydrogen bonding. The induction energy term and the dispersion energy term are nearly equal for the complex ClF−HF. For the ClF−H_2O and ClF−H_3N complexes, the induction energy is rather small, and the dispersion energy dominates.

3. For the X−Cl-type complex HF−ClF, the main interaction energy comes from the electrostatic energy, which slightly outweighs the exchange term. For the two strongest X−Cl-type complexes, H_2O−ClF and H_3N−ClF, the exchange energy outweighs the electrostatic energy but the large attractive induction and dispersion energies lead to a

very strong interaction. In the strongest N−Cl-type complex, H_3N−ClF, the induction energy is the most important attractive term, followed by the exchange and electrostatic energy, and is responsible for stabilizing the complex. This domination of the induction and exchange terms is the main feature of the strong and partly covalent bonds. This is also consistent with significant charge redistribution.

Acknowledgment. We are grateful to the Special Research Fund for the Doctoral Program of Higher Education (20050010014) for financial support. Authors would also like to thank Professor Krzysztof Szalewicz for providing the SAPT2002 program.

References

(1) Lehn, J. M. *Supramolecular Chemistry. Concepts and Perspectives*; VCH: Weinheim, Germany, 1995.

(2) Desiraju, G. R. *Crystal Engineering: The Design of Organic Solids*; Elsevier: Amsterdam, The Netherlands, 1989.

(3) Desiraju, G. R.; Steiner, T. *The Weak Hydrogen Bond In Structural Chemistry and Biology*; Oxford University Press: New York, 1997.

(4) Nishio, M.; Hirota, M.; Umezawa, Y. *The CH-Interaction*; Wiley-VCH: New York, 1998.

(5) Scheiner, S. *Molecular Interactions*: *From Van der Waals to Strong Bound Complexes*; Wiley: Chichester, U. K., 1997.

(6) Jeffrey, J. A.; Saenger, W. *Hydrogen Bonding in Biological Structures*; Springer-Verlag: Berlin, 1991.

(7) Umeyama, H.; Morokuma, K.; Yamabe, S. *J. Am. Chem. Soc.* **1977**, *99*, 330−343.

(8) Kollman, P.; Dearling, A.; Kochanski, E. *J. Phys. Chem.* **1982**, *86*, 1607−1614.

(9) Røeggen, I.; Dahl, T. *J. Am. Chem. Soc.* **1992**, *114*, 511−516.

(10) Price, S. L.; Stone, A. J.; Lucas, J.; Rowland, R. S.; Thornley, A. E. *J. Am. Chem. Soc.* **1994**, *116*, 4910−4918.

(11) (a) Legon, A. C.; Lister, D. G.; Thorn, J. C. *J. Chem. Soc. Chem. Commun.* **1994**, 757−758. (b) Legon, A. C.; Lister, D. G.; Thorn, J. C. *J. Chem. Soc., Faraday Trans.* **1994**, *90*, 3205−3212. (c) Bloemink, H. I.; Legon, A. C.; Thorn, J. C. *J. Chem. Soc., Faraday Trans.* **1994**, *90*, 781−787. (d) Legon, A. C. *Chem.—Eur. J.* **1998**, *4*, 1890−1897.

(12) Desiraju, G. R. *Angew. Chem., Int. Ed. Engl.* **1995**, *34*, 2311−2327.

(13) Latajka, Z.; Berski, S. *THEOCHEM* **1996**, *371*, 11−16.

(14) Ruiz, E.; Salahub, D. R.; Vela, A. *J. Phys. Chem.* **1996**, *100*, 12265−12276.

(15) Lommerse, J. P. M.; Stone, A. J.; Taylor, R.; Allen, F. H. *J. Am. Chem. Soc.* **1996**, *118*, 3108−3116.

(16) Bürger, H. *Angew. Chem., Int. Ed. Engl.* **1997**, *36*, 718−721.

(17) Zhang, Y.; Zhao, C.-Y.; You, X.-Z. *J. Phys. Chem. A.* **1997**, *101*, 2879−2885.

(18) Alkorta, I.; Rozas, I.; Elguero, J. *J. Phys. Chem. A.* **1998**, *102*, 9278−9285.

(19) Amico, V.; Meille, S. V.; Corradi, E.; Messina, M. T.; Resnati, G. *J. Am. Chem. Soc.* **1998**, *120*, 8261−8262.

(20) Farina, A.; Meille, S. V.; Messina, M. T.; Metrangolo, P.; Resnati, G.; Vecchio, G. *Angew. Chem., Int. Ed.* **1999**, *38*, 2433−2436.

(21) Legon, A. C., *Angew. Chem., Int. Ed.* **1999**, *38*, 2686−2714.

(22) Corradi, E.; Meille, S. V.; Messina, M. T.; Metrangolo, P.; Resnati, G. *Angew. Chem., Int. Ed.* **2000**, *39*, 1782−1786.

(23) Valerio, G.; Raos, G.; Meille, S. V.; Metrangolo, P.; Resnati, G. *J. Phys. Chem. A* **2000**, *104*, 1617−1620.

(24) Karpfen, A. *J. Phys. Chem. A* **2000**, *104*, 6871−6879.

(25) Walsh, R. B.; Clifford, W.; Padgett, C. W.; Metrangolo, P.; Resnati, G.; Hanks, T. W.; Pennington, W. T. *Cryst. Growth Des.* **2001**, *1*, 165−175.

(26) Metrangolo, P.; Resnati, G. *Chem.—Eur. J.* **2001**, *7*, 2511−2519.

(27) Romaniello, P.; Lelj, F. J. *J. Phys. Chem. A.* **2002**, *106*, 9114−9119.

(28) Nangia, A. *CrystEngComm.* **2002**, *17*, 1−6.

(29) Burton, D. D.; Fontana, F.; Metrangolo, P.; Pilatid, T.; Resnatic, G. *Tetrahedron Lett.* **2003**, *44*, 645−648.

(30) Wang, W. Z.; Wong, N. B.; Zheng, W. X.; Tian, A. M. *J. Phys. Chem. A* **2004**, *108*, 1799−1805.

(31) Reed, A. E.; Weinbold, F.; Curtiss, L. A.; Pochatko, D. J. *J. Chem. Phys.* **1986**, *84*, 5687−5705.

(32) (a) Gu, Y.; Kar, T.; Scheiner, S. *J. Am. Chem. Soc.* **1999**, *121*, 9411−9422. (b) Hobza, P.; Havlas, Z. *Chem. Rev.* **2000**, *100*, 4253−4264. (c) Hobza, P.; Havlas, Z. *Chem. Phys. Lett.* **1999**, *303*, 447−452. (d) Hermansson, K. *J. Phys. Chem. A* **2002**, *106*, 4695−4702. (e) Qian, W.; Krimm, S. *J. Phys. Chem. A* **2002**, *106*, 6628−6636. (f) Alabugin, I. V.; Manoharan, M.; Peabody, S.; Weinhold, F. *J. Am. Chem. Soc.* **2003**, *125*, 5973−5987.

(33) Jeziorski, B.; Moszynski, R.; Szalewicz, K. *Chem. Rev.* **1994**, *94*, 1887−1930.

(34) Jeziorski, B.; Moszynski, R.; Ratkiewicz, A.; Rybak, S.; Szalewicz, K.; Williams, H. L. In *Methods and Techniques in Computational Chemistry*: *METECC-94*; Clementi, E., Ed.; STEF: Cagliari, Italy, 1993; Vol. B, Medium Sized Systems, pp 79−129.

(35) Møller, C.; Plesset, M. S. *Phys. Rev.* **1934**, *46*, 618−622.

(36) Hobza, P.; S̈yponer, *J. Chem. Rev.* **1999**, *99*, 3247−3276.

(37) (a) Dunning, T. H., Jr. *J. Chem. Phys.* **1989**, *90*, 1007−1023. (b) Woon, D. E.; Dunning, T. H., Jr. *J. Chem. Phys.* **1993**, *98*, 1358−1364. It is well-known that the aug-cc-pVXZ series of basis sets was designed for frozen-core MP2 calculations. Here, we employed the aug-cc-pVTZ basis set for fully correlated calculations because our test calculations clearly showed that the values of the counterpoise-corrected binding energies obtained using fully correlated MP2 calculations are more close to their CBS limit values than those obtained using frozen-core MP2 calculations.

(38) Boys, S. F.; Bernardi, F. *Mol. Phys.* **1970**, *19*, 553−556.

(39) Simon, S.; Duran, M.; Dannenberg, J. J. *J. Chem. Phys.* **1996**, *105*, 11024−11031.

(40) Hobza, P.; Havlas, Z. *Theor. Chem. Acc.* **1998**, *99*, 372−377.

(41) Simon, S.; Duran, M.; Dannenberg, J. J. *J. Phys. Chem. A.* **1999**, *103*, 1640−1643.

(42) Karpfen, A. *J. Phys. Chem. A* **2000**, *104*, 6871−6879.

(43) (a) Reed, A. E.; Weinstock, R. B.; Weinhold, F. *J. Chem. Phys.* **1985**, *83*, 735−746. (b) Reed, A. E.; Weinstock, R. B.; Weinhold, F. *J. Chem. Phys.* **1985**, *83*, 1736−1740. (c) Reed, A. E.; Curitss, L. A.; Weinhold, F. *Chem. Rev.* **1988**, *88*, 889−926.

(44) Frisch, M. J.; Trucks, G. W.; Schlegel, H. B.; Scuseria, G. E.; Robb, M. A.; Cheeseman, J. R.; Montgomery, J. A., Jr.; Vreven, T.; Kudin, K. N.; Burant, J. C.; Millam, J. M.; Iyengar, S. S.; Tomasi, J.; Barone, V.; Mennucci, B.; Cossi, M.; Scalmani, G.; Rega, N.; Petersson, G. A.; Nakatsuji, H.; Hada, M.; Ehara, M.; Toyota, K.; Fukuda, R.; Hasegawa, J.; Ishida, M.; Nakajima, T.; Honda, Y.; Kitao, O.; Nakai, H.; Klene, M.; Li, X.; Knox, J. E.; Hratchian, H. P.; Cross, J. B.; Adamo, C.; Jaramillo, J.; Gomperts, R.; Stratmann, R. E.; Yazyev, O.; Austin, A. J.; Cammi, R.; Pomelli, C.; Ochterski, J. W.; Ayala, P. Y.; Morokuma, K.; Voth, G. A.; Salvador, P.; Dannenberg, J. J.; Zakrzewski, V. G.; Dapprich, S.; Daniels, A. D.; Strain, M. C.; Farkas, O.; Malick, D. K.; Rabuck, A. D.; Raghavachari, K.; Foresman, J. B.; Ortiz, J. V.; Cui, Q.; Baboul, A. G.; Clifford, S.; Cioslowski, J.; Stefanov, B. B.; Liu, G.; Liashenko, A.; Piskorz, P.; Komaromi, I.; Martin, R. L.; Fox, D. J.; Keith, T.; Al-Laham, M. A.; Peng, C. Y.; Nanayakkara, A.; Challacombe, M.; Gill, P. M. W.; Johnson, B.; Chen, W.; Wong, M. W.; Gonzalez, C.; Pople, J. A. *Gaussian 03*, Revision C.02; Gaussian, Inc.: Wallingford, CT, 2004.

(45) Lide, D. R. CRC *Handbook of Chemistry and Physics*, 73rd ed.; CRC Press: Boca Raton, FL, 1992.

(46) Williams, H. L.; Szalewicz, K.; Jeziorski, B.; Moszynski, R.; Rybak, S. *J. Chem. Phys.* **1994**, *98*, 1279−1291.

(47) (a) Moszynski, R.; Jeziorski, B.; Ratkiewicz, A.; Rybak, S. *J. Chem. Phys.* **1993**, *99*, 8856−8869. (b) Moszynski, R.; Jeziorski, B.; Rybak, S. *J. Chem. Phys.* **1994**, *100*, 1312−1325. (c) Moszynski, R.; Jeziorski, B.; Rybak, S.; Szalewicz, K.; Williams, H. L. *J. Chem. Phys.* **1994**, *100*, 5080−5092. (d) Rybak, S.; Jeziorski, B.; Szalewicz, K. *J. Chem. Phys.* **1995**, *95*, 6576−6610. (e) Moszynski, R.; Cybulski, S. M.; Chalasinski, G. *J. Chem. Phys.* **1994**, *100*, 4998−5010. (f) Chalasinski, G.; Jeziorski, B. *Theor. Chim. Acta* **1977**, *46*, 277−290. (g) Moszynski, R.; Korona, T.; Wormer, P. E. S.; van der Avoird, A. *J. Phys. Chem. A* **1997**, *101*, 4690−4698.

(48) Szalewicz, K.; Cole, S. J.; Kolos, W.; Bartlett, R. J. *J. Chem. Phys.* **1988**, *89*, 3662−3673.

(49) Bukowski, R.; Szalewicz, K.; Chabalowski, C. *J. Phys. Chem. A* **1999**, *103*, 7322−7340.

(50) Milet, A.; Moszynski, R.; Wormer, P. E. S.; van der Avoird, A. *J. Phys. Chem. A* **1999**, *103*, 6811−6819.

(51) Wormer, P. E. S.; van der Avoird, A. *Chem. Rev.* **2000**, *100*, 4109−4143.

(52) Kim, K. S.; Tarakeshwar, P.; Lee, J. Y. *Chem. Rev.* **2000**, *100*, 4145−4185.

(53) Bukowski, R.; Cencek, W.; Jankowski, P.; Jeziorski, B.; Jeziorska, M.; Kucharski, S. A.; Misquitta, A. J.; Moszynski, R.; Patkowski, K.; Rybak, S.; Szalewicz, K.; Williams, H. L.; Wormer, P. E. S. *SAPT2002: An Ab Initio Program for Many-Body Symmetry-Adapted Perturbation Theory Calculations of Intermolecular Interaction Energies. Sequential and Parallel Versions, 2003*.

CT600229N